Gene Therapy (2015) **22**, 104–110
© 2015 Macmillan Publishers Limited All rights reserved 0969-7128/15
www.nature.com/gt

SHORT COMMUNICATION

Noninvasive, neuron-specific gene therapy can be facilitated by focused ultrasound and recombinant adeno-associated virus

S Wang[1], OO Olumolade[1], T Sun[1], G Samiotaki[1] and EE Konofagou[1,2]

Recombinant adeno-associated virus (rAAV) has shown great promise as a potential cure for neurodegenerative diseases. The existence of the blood–brain barrier (BBB), however, hinders efficient delivery of the viral vectors. Direct infusion through craniotomy is the most commonly used approach to achieve rAAV delivery, which carries increased risks of infection and other complications. Here, we report a focused ultrasound (FUS)-facilitated noninvasive rAAV delivery paradigm that is capable of producing targeted and neuron-specific transductions. Oscillating ultrasound contrast agents (microbubbles), driven by FUS waves, temporarily 'unlock' the BBB, allowing the systemically administrated rAAVs to enter the brain parenchyma, while maintaining their bioactivity and selectivity. Taking the advantage of the neuron-specific promoter *synapsin*, rAAV gene expression was triggered almost exclusively (95%) in neurons of the targeted caudate–putamen region. Both behavioral assessment and histological examination revealed no significant long-term adverse effects (in the brain and several other critical organs) for this combined treatment paradigm. Results from this study demonstrated the feasibility and safety for the noninvasive, targeted rAAV delivery, which might have open a new avenue in gene therapy in both preclinical and clinical settings.

Gene Therapy (2015) **22,** 104–110; doi:10.1038/gt.2014.91; published online 6 November 2014

INTRODUCTION

The pathology of Parkinson's disease (PD) is characterized by the relatively selective death of neuronal subtypes, namely the nigrostriatal dopaminergic (DA) neurons.[1] Although the exact pathogenesis of PD is still under investigation, the discovery of the dopamine precursor L-dopa,[2] which can be taken up by the remaining DA neurons and converted to dopamine, alleviated symptoms for PD patients. Unfortunately, with ongoing loss of DA neurons, the uptake of extracellular L-dopa gradually declines. Alternatively, gene therapy was proposed as a means for achieving localized and prolonged transgene expression.[3] Until now, several clinical trials designed for PD patients were performed using recombinant adeno-associated virus serotype 2 (rAAV2) carrying various genomes: human aromatic acid decarboxylase;[4] glutamic acid decarboxylase;[5] and more recently neurturin.[6] Although all of these trials demonstrated tolerability of rAAV2 vectors in PD patients, the insignificant therapeutic effects might have resulted from limited injection sites and lack of an effective transduction volume. To overcome these limitations, multiple injections were administered. However, the increased number of injections poses higher risks in targeting accuracy, mechanical failure, infection and other complications for PD patients.[5,7] Moreover, given the relatively large molecular size of rAAV (~20 nm) and the high intracranial pressure,[8] the vectors are expected to remain in the proximity of the catheter tip,[9] leading to a suboptimal transduction volume.

Alternatively, rAAV could be administered systemically, and by adapting the design of viral vectors cell-specific transduction may be achieved. Nonetheless, the presence of the blood–brain barrier (BBB) prevents almost all large molecules (including rAAV) from entering the brain parenchyma.[10] Recent advances in therapeutic ultrasound and its application in BBB disruption provide a promising alternative for circumventing these obstacles.[11,12] The ultrasound beam can be focused at the targeted region (on the order of millimeters), causing oscillations of the systemically administered microbubbles. Focused ultrasound (FUS) in combination with microbubbles has been shown to be capable of noninvasively inducing reversible BBB opening in rodents, as well as in nonhuman primates.[13,14] Molecules of various sizes were successfully delivered to the brain: neurotropic factors,[15] antibodies[16] and chemotherapeutic agents.[17] Several efforts have been reported toward noninvasively delivering rAAV across the BBB for the purpose of gene therapy.[18–20] Among the reported studies, the neuron transduction rate (18–40%) was either significantly below the effective level or not quantified. In addition, no safety profile of the proposed treatment paradigm was adequately established and documented. Therefore, the goal of this study is to demonstrate the feasibility of FUS-facilitated, neuron-specific rAAV transduction, and to establish its safety profiles.

RESULTS AND DISCUSSION

The caudate–putamen (CPu) was chosen as the primary target for FUS-induced BBB opening because it is directly linked to motor functions of the animal model used in this study. The acoustic beam was tightly focused (with a −6-dB pressure volume of $1 \times 1 \times 7\ mm^3$) through a coupling medium onto the intended target. A mixture of rAAV–synapsin–GFP (either serotype 1 or 2) and in-house-manufactured microbubbles (mean diameter of

[1]Ultrasound and Elasticity Imaging Laboratory, Department of Biomedical Engineering, Columbia University, New York, NY, USA and [2]Department of Radiology, Columbia University, New York, NY, USA. Correspondence: Dr EE Konofagou, Ultrasound and Elasticity Imaging Laboratory, Department of Biomedical Engineering, Columbia University, 351 Engineering Terrace, Mail Code 8904, 1210 Amsterdam Avenue, New York, NY 10027, USA.
E-mail: ek2191@columbia.edu
Received 18 April 2014; revised 30 July 2014; accepted 26 August 2014; published online 6 November 2014

0.9 μm) was administered via the tail vein immediately before sonication. The oscillation of microbubbles (driven by the ultrasound field) was monitored with a passive cavitation detector, and the cavitation dose was quantified (Figure 1a) for each group as an indicator for bubble–blood vessel wall interactions. The cavitation doses of the BBB opened groups were significantly higher ($P < 0.001$ for rAAV1 and $P < 0.01$ for rAAV2) compared to those the control. The temporary opening of the BBB was confirmed with T1-weighted contrast-enhanced magnetic resonance imaging (MRI). The contrast agent gadodiamide (MW 573.66 Da) does not cross the BBB under normal, physiological conditions. However, the BBB opened region (namely, left CPu) was highlighted by the diffusion of gadodiamide (Figure 1b), indicating localized BBB opening. The diffusion of the MR contrast agent was clearly revealed as the bright region from the reconstructed three-dimensional MR image (Figure 1c).

Mice were killed 4 weeks after the initial sonication. The coronally sectioned brain slices were stained for neurons and astrocytes with anti-NeuN and anti-GFAP antibodies, respectively. By comparing the FUS-treated side against the contralateral side (which served as a rAAV-only control), as shown in Figure 1d, significant transgene expression (GFP) was observed on the BBB opened side, whereas the contralateral side was virtually free of rAAV transduction. We also identified the types of transduced cells using a customized image processing algorithm on the basis of the fluorescent images. It was found that for both types of rAAVs ~95% (96.3 ± 1.9% for rAAV1 and 93.7 ± 2.4% for rAAV2) of the transduced cells were neurons (Figure 1e). In addition, transductions of astrocytes and unidentified cells were also observed, although to a lesser degree (that is, altogether ~5%). Magnification of transgene-expressing neurons and astrocytes is shown in Figure 1f. Such neuron-specific transduction was achieved primarily by the viral *promoter synapsin* for both rAAV1 and rAAV2 vectors. Kügler *et al.*[21] reported that the transgene expression from adenoviral vectors (directly infused into the rat brain) can be restricted exclusively to neurons by using a small fragment of the human synapsin 1 gene. In this study, we demonstrated that systemically administered rAAV1 and rAAV2 with synapsin promoter also exhibited neuron-specific transduction once across the BBB.

We quantified the distribution of the rAAV transduction in the targeted CPu region. As shown in Figure 2a, GFP was stained in brown color using the ABC-DAB method. The rAAV1 (Figure 2a left column)-transduced cells (dark brown) can be clearly observed on the left side (FUS treated) of the brain sections (corresponding to sections 2, 4 and 6 in Figure 2b), whereas rAAV2 presented much lower transduction efficiency (Figure 2a right column, corresponding to sections 4, 6, 8 in Figure 2c). The contralateral side

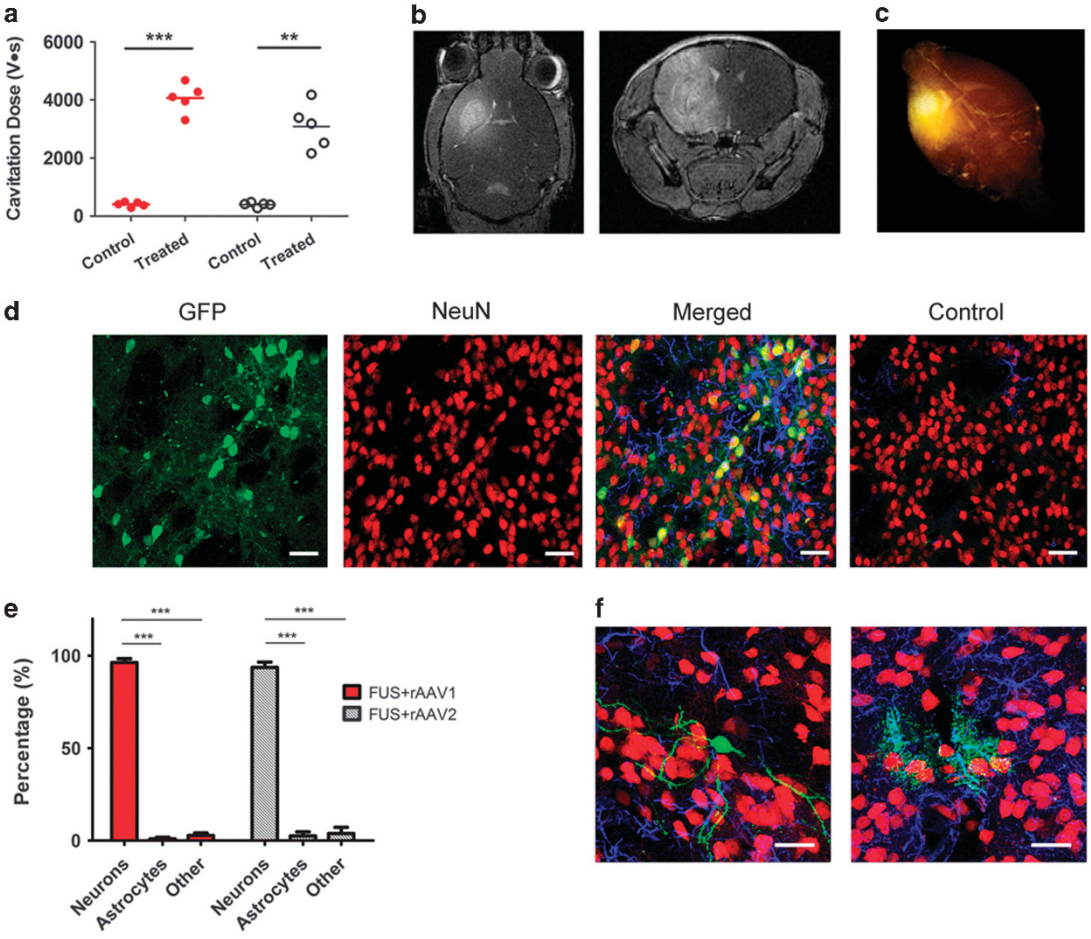

Figure 1. Targeted BBB disruption is achieved by FUS and microbubbles, and the transgene is primarily expressed in neurons. (**a**) Increased cavitation doses, indicating microbubble–blood vessel interaction, were found in FUS-treated groups (red: rAAV1; black: rAAV2). (**b**) Contrast-enhanced T1-weighted MR images revealed targeted BBB disruption (highlighted region). (**c**) The bright region from the three-dimensional reconstructed mouse brain image revealed the volume of the BBB opening. (**d**) Transgene expression was found only in the FUS-treated region. The colocalization of GFP-positive and NeuN-positive cells indicates neuron-specific transduction. Scale bars, 20 μm. (**e**) Transgene expression was almost exclusively restricted in neurons, and only ~5% of transduced cells were astrocytes and unidentified cells. (**f**) Examples of transgene expression in a neuron and an astrocyte. Scale bars, 20 μm. $^{**}P < 0.01$, $^{***}P < 0.001$ by unpaired *t*-test. Error bars indicate s.d.

© 2015 Macmillan Publishers Limited

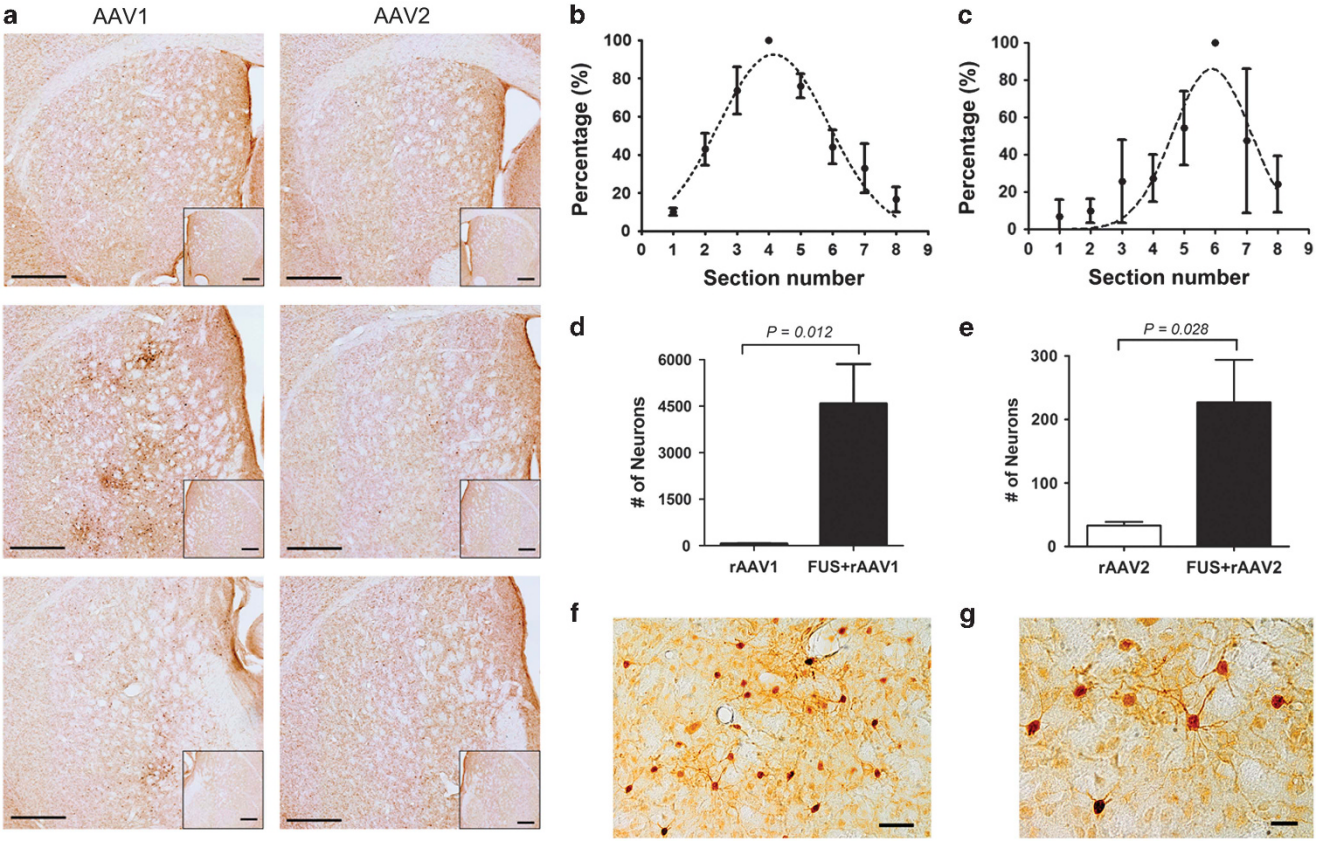

Figure 2. FUS-facilitated rAAV delivery is localized, and rAAV1 exhibits more efficient transduction than rAAV2. (**a**) Examples of rAAV1 and rAAV2 transgene expression (dark brown) in the targeted region (left CPu). The inter-section distance was 440 μm. The contralateral side of the brain is shown in the black square at the bottom right corner of each image. Scale bars, 500 μm. (**b** and **c**) Normalized numbers of rAAV1- (**b**) and rAAV2 (**c**)-transduced cells revealed Gaussian distributions, corresponding to the profile of the FUS pressure field in the radial direction. The FUS-treated side showed a significantly higher number of transduced cells than the contralateral side for both rAAV1 (**d**) and rAAV2 (**e**). (**f** and **g**) Magnified bright-field images revealing rAAV transgene expression. Scale bars, 50 μm (**f**) and 20 μm (**g**).

(untreated, right bottom corner of each image in Figure 2a) showed minimal or no rAAV transduction. The total number of transgene-expressing neurons was quantified with a custom-built algorithm, which was validated with manual counting (discrepancy was within 15%). For each brain, eight sections (thickness of 40 μm), which had an inter-sectional space of 200 μm, were stained and quantified. The number of rAAV-transduced neurons for each section was normalized against the maximum neuron count of each brain. As shown in Figures 2b and c, the transduced neurons followed a Gaussian distribution for both rAAV1- and rAAV2-treated groups ($R^2 = 0.7594$ and 0.6504, respectively). This was caused by the circular shape of the FUS beam in the radial dimension. In other words, the acoustic pressure field also exhibited a Gaussian distribution in the transverse direction, intrinsically resulting from the focusing geometry of the FUS beam. As shown in Figure 2d, the total number of rAAV1-transduced neurons in the CPu region, with a single sonication, was estimated to be 4581 ± 2005, which is significantly higher compared with the contralateral side ($P = 0.012$). The number of rAAV2-transduced neurons on the treated side, although significantly higher ($P = 0.028$) than the contralateral side, is much less effective than that of the rAAV1-treated groups ($P = 0.014$). A magnified observation of the bright-field images is given in Figures 2f and g, where the soma and dendrites of the transduced neurons are clearly marked with dark brown color.

We have investigated the long-term safety aspects of the proposed treatment paradigm with both histological examinations and behavioral tests. One concern for the systemically administered rAAV vectors was transduction in unintended organs. To address this concern, four critical organs (heart, lung, liver and kidney) from each mouse were harvested after killing. The organs were then sectioned at 20 μm and imaged for transgene expression (GFP). As shown in Figure 3a, no increased GFP signal was observed from the rAAV-treated groups when compared with the sham group. Histological examinations were performed using mice treated with FUS only, as rAAV vectors have been shown to be safe and tolerable in clinical trials.[6,22,23] After initial treatment, these mice were killed following a survival time of 4 weeks (to be consistent with the rAAV+FUS-treated groups). On the basis of the hematoxylin and eosin staining and Nissl staining results, no long-term brain damage was observed in either the FUS-treated region or the contralateral side (Figures 3b and c).

As the FUS-targeted region was the CPu, which is closely linked to motor functions, the rotarod performance test and the vertical pole test were selected to monitor potential alterations in behavior.[24] The tests were repeated on a weekly basis for rAAV1 +FUS-treated, rAAV2+FUS-treated and sham groups until the end of the survival period. No significant change was observed between these groups from the vertical pole test, shown in Figure 3d. There was, however, a statistically significant difference ($P < 0.05$) between week 0 and week 3 within the rAAV2-treated group. This may be attributed to the learning curve of the animals, as the same trend can be found in the other two groups (although not significant). Furthermore, the rotarod test (shown in Figure 3e) showed no significant difference between the rAAV+FUS-treated groups and the sham group from each week. These observations demonstrated that, from both behavioral and histological aspects,

© 2015 Macmillan Publishers Limited

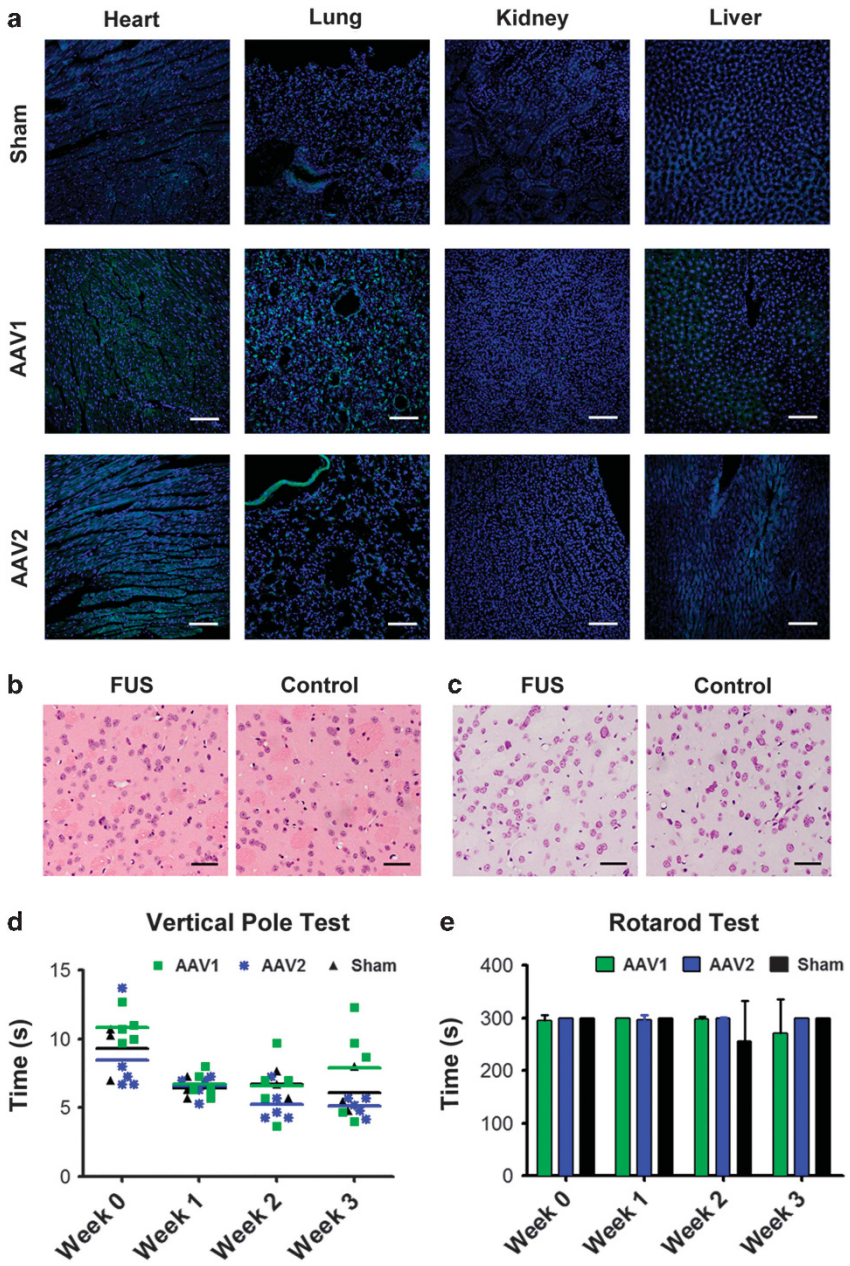

Figure 3. The combined FUS and rAAV treatment showed no significant adverse effect *in vivo*. (**a**) Fluorescent images of the heart, lung, kidney and liver showed no rAAV transduction when compared with sham. Scale bars, 100 μm. (**b**) Hematoxylin and eosin staining and (**c**) Nissl staining of the FUS-treated brains showed no long-term cellular damage. Scale bars, 60 μm. (**d** and **e**) No significant change was observed across the 4-week survival period from the vertical poll test (**d**) and the rotarod performance test (**e**).

the combined rAAV- and FUS-induced BBB opening paradigm is safe for the noninvasive and targeted gene therapy.

Gene therapy has been proposed for the treatment of neurodegenerative diseases for its persistent transgene expression. Among all gene therapeutic vehicles, rAAV has shown great potential, especially regarding its safety and tolerability profile from clinical trials. Conventionally, these vectors are infused through a cannula directly into the targeted brain region, and convection-enhanced delivery systems were then developed to increase the diffusion volume.[9] More recently, novel cannulae were proposed to further enhance the delivery efficiency. For instance, a micro-fabricated catheter with MR compatibility was evaluated *in vivo* for intraparenchymal delivery;[25] a radially branched cannula was designed for efficient delivery at the scale of the human brain.[26] Nevertheless, all cannula-based approaches require invasive procedures and may cause various complications. Here, we propose a noninvasive, targeted and neuron-specific gene therapy paradigm using FUS and rAAV vectors with the *synapsin* promoter. Our approach, unlike the cannula-based delivery systems, is capable of achieving completely noninvasive rAAV delivery to the brain. More importantly, this technique allows flexible implementation of multisite delivery by simply repositioning the FUS transducer.

One limitation of this study is that the FUS sonication and rAAV administration were carried out in mice at a relatively young age (10 weeks old). Nevertheless, successful repeated FUS-induced BBB openings have been reported in nonhuman primates over periods as long as 13 months.[27,28] Compared with cannula-based approaches, our technique required a higher dose of intravenously administered viral vectors while the optimal dose needs to

© 2015 Macmillan Publishers Limited

be determined in future studies. By selecting appropriate promoters, nonspecific transduction can be minimized and no long-term adverse effects were observed from behavioral tests and histological examinations. The results presented here demonstrated the feasibility and safety of a noninvasive and neuron-specific gene therapy approach.

MATERIALS AND METHODS

Animal preparation

All experimental procedures involving animals were approved by the Columbia University Institutional Animal Care and Use Committee. A total of 18 mice (age 10 weeks) were used in this study and were divided into four groups: FUS+rAAV1 ($n=5$), FUS +rAAV2 ($n=5$), FUS only ($n=5$) and sham ($n=3$). Mice were anesthetized with a mixture of oxygen and 1–2% isoflurane (SurgiVet, Smiths Medical PM, Inc., Dublin, OH, USA) and placed prone with its head immobilized by a stereotaxic apparatus (David Kopf Instruments, Tujunga, CA, USA). The scalp fur was removed using an electrical trimmer and depilatory cream to minimize acoustic impedance mismatch.

Microbubble and rAAV vectors

Microbubbles were manufactured in-house according to the previously published protocol.[29] Briefly, the 1,2-distearoyl-sn-glycero-3-phosphocholine and polyethylene Glycol 2000 (PEG2000) were mixed at a 9:1 ratio. Two milligrams of the mixture was dissolved in a 2- ml solution consisting of filtered phosphate-buffered saline/glycerol (10% volume)/propylene glycol (10% volume) using a sonicator (Model 1510, Branson Ultrasonics, Danbury, CT, USA) and stored in a 5 -ml vial at 4 °C. The empty space of the vial was filled with decafluorobutane gas and activated via mechanical agitation using VialMix (Lantheus Medical Imaging, N. Billerica, MA, USA) shaker for a preset time of 45 s. The concentration and size distribution of each microbubble vial were measured with a Coulter Counter Multisizer (Beckman Coulter Inc., Fullerton, CA, USA).

The rAAV vectors used in this study were purchased from SignaGen Laboratories (Rockville, MD, USA). Both rAAV1- and rAAV2-expressing eGFP under the control of *synapsin* promoter were used. The titer of the viral vectors was provided by the manufacturer (quantified with real-time PCR) and diluted in phosphate-buffered saline to 1.1×10^{12} GC ml^{-1}. For each mouse (average body weight of 25 g), a total of 100 µl of diluted rAAV was mixed with $\sim 2.5\times10^{7}$ microbubbles and injected via the tail vein.

FUS

The FUS sonications were carried out with a single-element focused transducer (focal length: 60 mm, and radius: 30 mm, Imasonic, France), which has a center frequency of 1.5 MHz. The −6-dB pressure focal zone of the FUS transducer was measured using a needle hydrophone (Precision Acoustics Ltd., Dorchester, UK) in degassed water to be $7.5\times1\times1$ mm^3. A confocally mounted pulse-echo transducer (radius: 11.2 mm, focal length: 60 mm and center frequency: 10 MHz; Olympus NDT, Waltham, MA, USA) was used for targeting and receiving cavitation signal during the treatments.[30] The pulse-echo transducer was driven by a pulser-receiver (Olympus), which was connected to a digitizer (Gage Applied Technologies, Inc., Lachine, QC, Canada) for data acquisition. The transducer cone was filled with deionized and degassed water and sealed with a piece of polyurethane membrane (Trojan; Church & Dwight Co., Inc., Princeton, NJ, USA). The FUS transducer was connected to a matching circuit and driven by a computer-controlled function generator (Agilent, Palo Alto, CA, USA) and 50 dB power amplifier (ENI Inc., Rochester, NY, USA). The transducer system was then mounted onto a computer-controlled three-dimensional positioner (Velmex Inc., Lachine, QC, Canada).

The intended target in this study was the CPu, and the targeting was achieved using a metallic grid approach, as described in previous reports.[30,31] Briefly, a metallic grid was placed on top of lambda, and the center of the grid was found from the reflected ultrasound signal. The FUS transducer was then moved according to the following coordinates: AP +6 mm and ML −2 mm. The center of the FUS focus was placed 3 mm below the skull, and 30% attenuation was accounted for acoustic pressure loss through the skull. An estimated *in situ* peak rarefactional pressure of 0.45 MPa was used for all sonications with a pulsing sequence of pulse repetition frequency 5 Hz, pulse length 20 ms and a total duration of 300 s. The rAAV and microbubble mixture was administered as a bolus via the tail vein immediately before the sonication. The cavitation signals were recorded by the pulse-echo transducer and the cavitation dose was quantified from the fast Fourier-transformed spectra (4–12 MHz) of each pulse with a custom-written program (MATLAB R2011a, MathWorks, Inc., Natick, MA, USA). The net cavitation emission from the contrast microbubbles was determined by subtracting the background signal measured using the identical ultrasound exposure before the microbubble administration.

MRI

MRI was performed for the FUS-only group upon completion of the FUS treatment. The BBB opening was confirmed with a 9.4T MRI system (Bruker Medical, Boston, MA, USA). The mice were placed in a birdcage coil (diameter 3 cm), while being anesthetized with 1–2% isoflurane, and vital sign was monitored throughout the imaging sessions. A bolus of 0.3 ml of gadodiamide (GD-DTPA) (Omniscan, GE Healthcare, Princeton, NJ, USA) was injected intraperitoneally into each mouse. Approximately 50 min post injection, MR images were collected using a contrast-enhanced T1-weighted two-dimensional FLASH sequence.[32]

Behavioral testing

To assess the safety of the BBB opening and rAAV systemic delivery, two types of behavior testing were performed: rotarod performance test and vertical pole test. The rotarod apparatus (Med Associates, St Albans, VT, USA) is composed of a plastic rod (32 mm in diameter) and a motion sensor underneath the rod. Each mouse was placed on the accelerating rod (initially at rest, acceleration 4 revolution min^{-2}) and allowed to stay on the rod for a maximum of 3 min. Falling off the rotarod, as well as latching onto the rotarod (rotating with the rod) for two consecutive revolutions, was considered the end of a trial. The vertical pole test was carried out using a rough-surfaced pole (length 80 cm). The mice were positioned upward on the pole, and the time for the mice to climb down was recorded. For both tests, three trials were conducted for each mouse, and the average value was used for analysis. The rAAV1, rAAV2 and sham groups underwent initial training for both tests (week 0) before the beginning of the FUS treatment. The testing was repeated on a weekly basis for each mouse until the end-point of the survival period (week 3).

Immunohistochemistry and histology

Mice were killed and transcardially perfused with 30 ml of phosphate-buffered saline, followed by 60 ml of 4% paraformaldehyde. The brains, as well as several critical organs (that is, heart, lung, liver, and kidney), were collected and soaked in paraformaldehyde. The skull was removed from the brains 24 h later, and the brains were fixed for one additional day. All tissues were cryoprotected with gradient sucrose solution (10% for 1 h, 20% for 2 h and 30% for overnight), frozen on dry ice and kept in a −80 °C freezer. The brain samples were sectioned coronally at 40 µm, and

© 2015 Macmillan Publishers Limited

the entire CPu region was collected. For immunohistochemistry staining, every sixth section was treated with anti-GFP antibody (dilution 1:5000, Novus Biologicals, Littleton, CO, USA) and stained using the ABC-DAB method. The samples were then imaged with a bright-field microscope (Olympus, Center Valley, PA, USA). To identify the AAV-transduced cell type, immunofluorescent stainings were also carried out. The brain sections were incubated with primary antibodies: mouse anti-NeuN (dilution 1:200, Millipore, Temecula, CA, USA) and rabbit anti-GFAP (dilution 1:200, Invitrogen, Camarillo, CA, USA). The samples were then stained with fluorescently labeled secondary antibodies goat anti-mouse conjugated with Cy3 (dilution 1:200, Millipore) and goat anti-rabbit conjugated with Cy5 (dilution 1:200, Invitrogen). Fluorescent images were obtained with a confocal laser scanning microscope (Leica, Buffalo Grove, IL, USA). Paraffin-embedded brains (from the FUS only group) were sectioned at 7 μm and used for hematoxylin and eosin staining. The organs were sectioned at 20 μm in thickness and stained with DAPI upon imaging. The images were taken with a Nikon confocal microscope (Nikon Instruments Inc., Melville, NY, USA).

Image analysis

All image analyses were carried out using custom-written programs in MATLAB (R2011a, MathWorks, Inc., Natick, MA, USA). To identify the rAAV-transduced cell types, ten *Z*-stacked fluorescent images (of GFP, NeuN and GFAP channels) were taken from each brain. The maximum-projected GFP channel images were loaded into the program and used as the base for locating GFP-positive cells. Once a GFP-positive cell is identified by thresholding the grayscale images, the locations of its pixels were recorded. The intensity of these pixels from the NeuN channel and GFAP channel were quantified and determined to be NeuN positive or GFAP positive if at least 70% of the pixels were above the threshold. The total number of neurons for each brain was quantified on the basis of the DAB-stained sections (8 sections per brain with inter-sectional space of 200 μm). The bright-field images were first converted into grayscale format and the transduced cells were segmented. The results (from three different brains) from automatic counting program were compared with manual counting results, and the discrepancy was within 15%.

Statistics

Comparison between the two groups was made using two-tailed unpaired Student's *t*-test, and a *P*-value < 0.05 was considered to be statistically significant. Comparisons between the groups in behavioral testing were performed using one-way analysis of variance followed by the Bonferroni's *post-hoc* test.

CONFLICT OF INTEREST

The authors declare no conflict of interest.

ACKNOWLEDGEMENTS

This work was supported in part by NIH R01EB009041, NIH R01AG038961 and the Kinetics Foundation. We thank C Chen and H Chen for insightful discussion and comments. We also appreciate the assistance of Y Han and C Acosta in generating MRI and fluorescent images.

REFERENCES

1 Hirsch EC, Jenner P, Przedborski S. Pathogenesis of Parkinson's disease. *Mov Disord* 2013; **28**: 24–30.
2 Carlsson A. A half-century of neurotransmitter research: impact on neurology and psychiatry. Nobel lecture. *Biosci Rep* 2001; **21**: 691–710.
3 Chtarto A, Bockstael O, Tshibangu T, Dewitte O, Levivier M, Tenenbaum L. A next step in adeno-associated virus-mediated gene therapy for neurological diseases: regulation and targeting. *Br J Clin Pharmacol* 2013; **76**: 217–232.
4 Christine CW, Starr PA, Larson PS, Eberling JL, Jagust WJ, Hawkins RA *et al.* Safety and tolerability of putaminal AADC gene therapy for Parkinson disease. *Neurology* 2009; **73**: 1662–1669.
5 LeWitt Pa, Rezai AR, Leehey Ma, Ojemann SG, Flaherty AW, Eskandar EN *et al.* AAV2-GAD gene therapy for advanced Parkinson's disease: a double-blind, sham-surgery controlled, randomised trial. *Lancet Neurol* 2011; **10**: 309–319.
6 Bartus RT, Baumann TL, Siffert J, Herzog CD, Alterman R, Boulis N *et al.* Safety/feasibility of targeting the substantia nigra with AAV2-neurturin in Parkinson patients. *Neurology* 2013; **80**: 1698–1701.
7 Janson C, McPhee S, Bilaniuk L, Haselgrove J, Testaiuti M, Freese A *et al.* Clinical protocol. Gene therapy of Canavan disease: AAV-2 vector for neurosurgical delivery of aspartoacylase gene (ASPA) to the human brain. *Hum Gene Ther* 2002; **13**: 1391–1412.
8 Mann JD, Butler AB, Rosenthal JE, Maffeo CJ, Johnson RN, Bass NH. Regulation of intracranial pressure in rat, dog, and man. *Ann Neurol* 1978; **3**: 156–165.
9 Bobo RH, Laske DW, Akbasak A, Morrison PF, Dedrick RL, Oldfield EH. Convection-enhanced delivery of macromolecules in the brain. *Proc Natl Acad Sci USA* 1994; **91**: 2076–2080.
10 Abbott NJ. Blood-brain barrier structure and function and the challenges for CNS drug delivery. *J Inherit Metab Dis* 2013; **36**: 437–449.
11 Hynynen K, McDannold N, Sheikov Na, Jolesz Fa, Vykhodtseva N. Local and reversible blood-brain barrier disruption by noninvasive focused ultrasound at frequencies suitable for trans-skull sonications. *Neuroimage* 2005; **24**: 12–20.
12 Choi JJ, Selert K, Vlachos F, Wong A, Konofagou EE. Noninvasive and localized neuronal delivery using short ultrasonic pulses and microbubbles. *Proc Natl Acad Sci USA* 2011; **108**: 16539–16544.
13 McDannold N, Vykhodtseva N, Hynynen K. Targeted disruption of the blood–brain barrier with focused ultrasound: association with cavitation activity. *Phys Med Biol* 2006; **51**: 793–807.
14 Tung Y-S, Marquet F, Teichert T, Ferrera V, Konofagou EE. Feasibility of noninvasive cavitation-guided blood-brain barrier opening using focused ultrasound and microbubbles in nonhuman primates. *Appl Phys Lett* 2011; **98**: 163704.
15 Baseri B, Choi JJ, Deffieux T, Samiotaki G, Tung Y-S, Olumolade O *et al.* Activation of signaling pathways following localized delivery of systemically administered neurotrophic factors across the blood-brain barrier using focused ultrasound and microbubbles. *Phys Med Biol* 2012; **57**: N65–N81.
16 Jordão JF, Thévenot E, Markham-Coultes K, Scarcelli T, Weng Y-Q, Xhima K *et al.* Amyloid-β plaque reduction, endogenous antibody delivery and glial activation by brain-targeted, transcranial focused ultrasound. *Exp Neurol* 2013; 1–14.
17 Park E-J, Zhang Y-Z, Vykhodtseva N, McDannold N. Ultrasound-mediated blood-brain/blood-tumor barrier disruption improves outcomes with trastuzumab in a breast cancer brain metastasis model. *J Control Release* 2012; **163**: 277–284.
18 Thévenot E, Jordão JF, O'Reilly MA, Markham K, Weng Y-Q, Foust KD *et al.* Targeted delivery of self-complementary adeno-associated virus serotype 9 to the brain, using magnetic resonance imaging-guided focused ultrasound. *Hum Gene Ther* 2012; **23**: 1144–1155.
19 Alonso A, Reinz E, Leuchs B, Kleinschmidt J, Fatar M, Geers B *et al.* Focal delivery of AAV2/1-transgenes into the rat brain by localized ultrasound-induced BBB opening. *Mol Ther Nucleic Acids* 2013; **2**: e73.
20 Hsu P-H, Wei K-C, Huang C-Y, Wen C-J, Yen T-C, Liu C-L *et al.* Noninvasive and targeted gene delivery into the brain using microbubble-facilitated focused ultrasound. *PLoS One* 2013; **8**: e57682.
21 Kügler S, Kilic E, Bähr M. Human synapsin 1 gene promoter confers highly neuron-specific long-term transgene expression from an adenoviral vector in the adult rat brain depending on the transduced area. *Gene Ther* 2003; **10**: 337–347.
22 Salegio EA, Samaranch L, Jenkins RW, Clarke CJ, Lamarre C, Beyer J *et al.* Safety study of adeno-associated virus serotype 2-mediated human acid sphingomyelinase expression in the nonhuman primate brain. *Hum Gene Ther* 2012; **23**: 891–902.
23 Kaplitt MG, Feigin A, Tang C, Fitzsimons HL, Mattis P, Lawlor PA *et al.* Safety and tolerability of gene therapy with an adeno-associated virus (AAV) borne GAD gene for Parkinson's disease: an open label, phase I trial. *Lancet* 2007; **369**: 2097–2105.
24 Brooks SP, Dunnett SB. Tests to assess motor phenotype in mice: a user's guide. *Nat Rev Neurosci* 2009; **10**: 519–529.
25 Brady ML, Raghavan R, Singh D, Anand PJ, Fleisher AS, Mata J *et al.* In vivo performance of a microfabricated catheter for intraparenchymal delivery. *J Neurosci Methods* 2014; **229**: 76–83.
26 Silvestrini MT, Yin D, Coppes VG, Mann P, Martin AJ, Larson PS *et al.* Radially branched deployment for more efficient cell transplantation at the scale of the human brain. *Stereotact Funct Neurosurg* 2013; **91**: 92–103.

© 2015 Macmillan Publishers Limited

27 McDannold N, Arvanitis CD, Vykhodtseva N, Livingstone MS. Temporary disruption of the blood-brain barrier by use of ultrasound and microbubbles: safety and efficacy evaluation in rhesus macaques. *Cancer Res* 2012; **72**: 3652–3663.
28 Downs ME, Buch A, Wu S-Y, Sierra C, Karakatsani M, Chen S *et al*. Safety of long term chronic blood brain barrier opening via microbubble enhanced focused ultrasound in non-human primates. *Fourth International Focused Ultrasound Symposium;* 12–16 October; Washington, DC, 2014.
29 Wang S, Samiotaki G, Olumolade O, Feshitan JA, Konofaqou EE. Microbubble type and distribution dependence of focused ultrasound-induced blood-brain barrier opening. *Ultrsound Med Biol* 2013; **40**: 1–8.
30 Tung Y-S, Vlachos F, Feshitan JA, Borden MA, Konofagou EE. The mechanism of interaction between focused ultrasound and microbubbles in blood-brain barrier opening in mice. *J Acoust Soc Am* 2011; **130**: 3059–3067.
31 Choi JJ, Pernot M, Brown TR, Small SA, Konofagou EE. Spatio-temporal analysis of molecular delivery through the blood–brain barrier using focused ultrasound. *Phys Med Biol* 2007; **52**: 5509–5530.
32 Vlachos F, Tung Y-S, Konofagou EE. Permeability assessment of the focused ultrasound-induced blood–brain barrier opening using dynamic contrast-enhanced MRI. *Phys Med Biol* 2010; **55**: 5451–5466.

© 2015 Macmillan Publishers Limited